

# Tracer Analysis by Mesoscale Field Experiments with 4D-var Data Assimilation

## SATEC4D



Hendrik Elbern, Achim Strunk

www.eurad.uni-koeln.de

Rhenish Institute for Environmental Research at the University of Cologne



### Introduction

SATEC4D aims to satisfy the frequently enunciated need to combine data with models on the highest possible sophistication level. Advanced space-time data assimilation methodology is the optimal choice. In practice, the four-dimensional variational (4d-var) data assimilation algorithm, which implies the development of the adjoint models, is an ambitious, yet computationally feasible option. It satisfies the optimality condition of a Best Linear Unbiased Estimator (BLUE), while a consistent evolution of the chemical state of the observed and modelled system is attained. The underlying chemistry transport model (CTM) is the EURAD (EUropean Air pollution Dispersion model), that is a state of the art continental to local scale air quality model.

### Objectives

Intending roughly a one campaign assimilation per year schedule, the following studies are involved in the project: **BERLIOZ** (prior to available AFO campaign data, PBL); **CONTRACE I** (UT); **SPURT IOP2** (UT/LS); **VERTIKO I** (PBL) and **ReHaTrop** (PBL).

After three years of this five years project, assimilation results from the first three campaigns are presented. In addition to the production of assimilation-based analyses, projects mentioned above are furnished with chemical forecasts for desired campaigns.

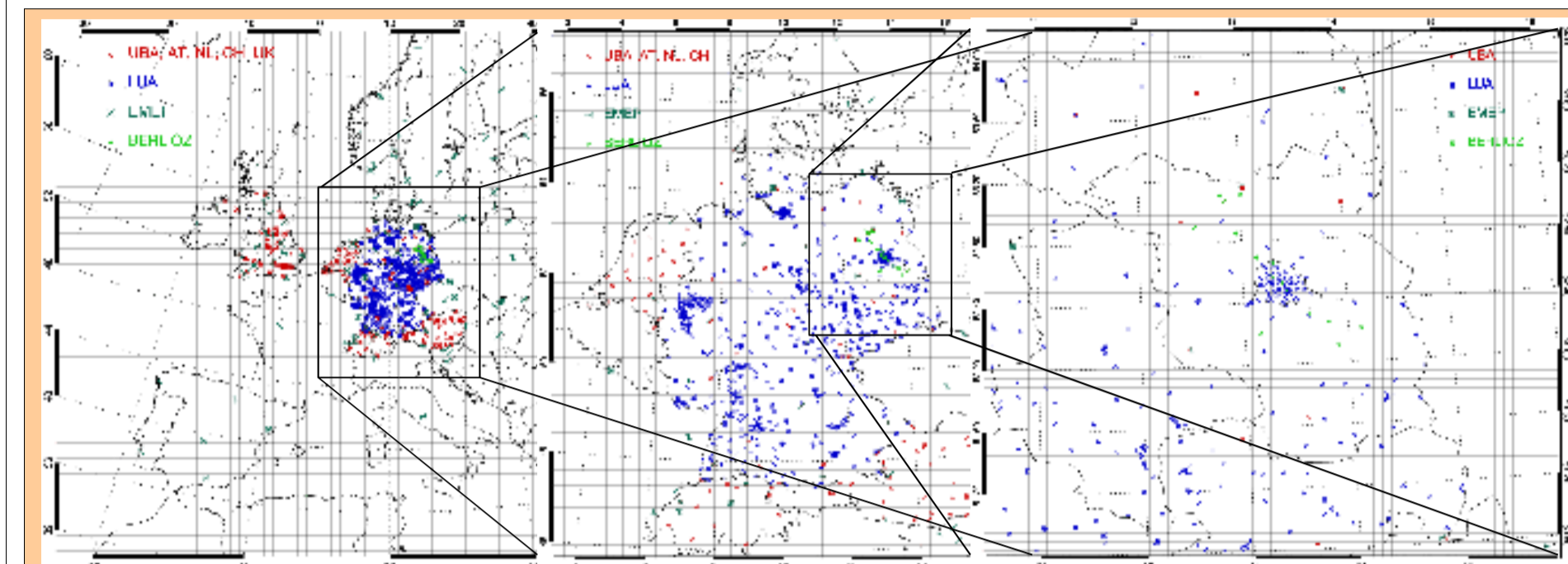


Figure 1: Nesting configuration and observation locations for BERLIOZ (from left to right): Coarse Grid (54 km), nest 1 (18 km), nest 2 (6 km).

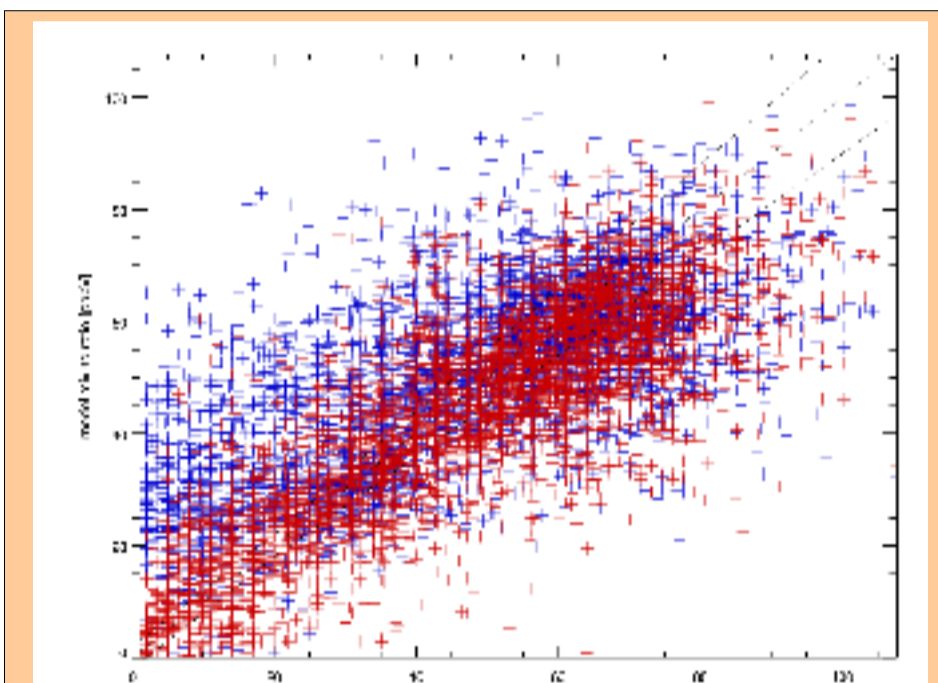


Figure 2: Ozone scatter (CG): first guess (blue), analysis (red).

### Survey of assimilation system achievements

The first developed chemistry 4d-var data assimilation system in the troposphere was the starting point for SATEC4D. During the project time the following principal achievements were attained:

- Generalisation of the optimisation parameter to emission rates, together with chemical state variables (see **BERLIOZ** and **CONTRACE**),
  - 4D-var multiple nesting with adjoint modelling (see **BERLIOZ**).
- Further advancements include the ingestion of data stemming from radio sondes and tethered balloons (figure 5), LIDAR, aircraft, satellite ozone profiles and NO<sub>2</sub> tropospheric column retrievals (figures 12 and 13). The horizontal and vertical grid design is kept optional. As far as verification data is available, success of data assimilation is verified by improved forecasts.

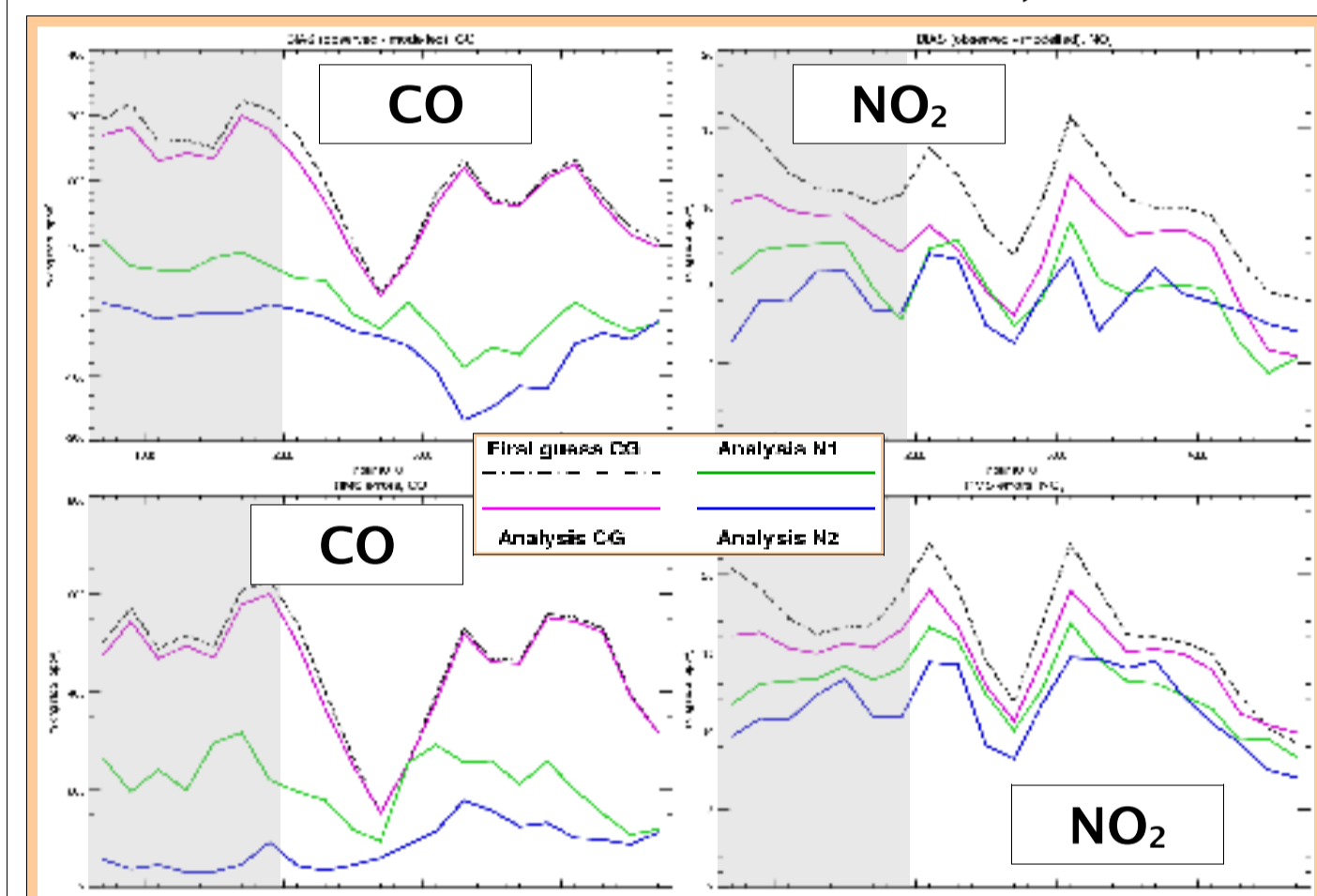


Figure 3: Nesting success: The two panels show BIAS and RMS error for CO and NO<sub>2</sub> in the 3 different grids. Shaded region: observations used for assimilation (assimilation interval).

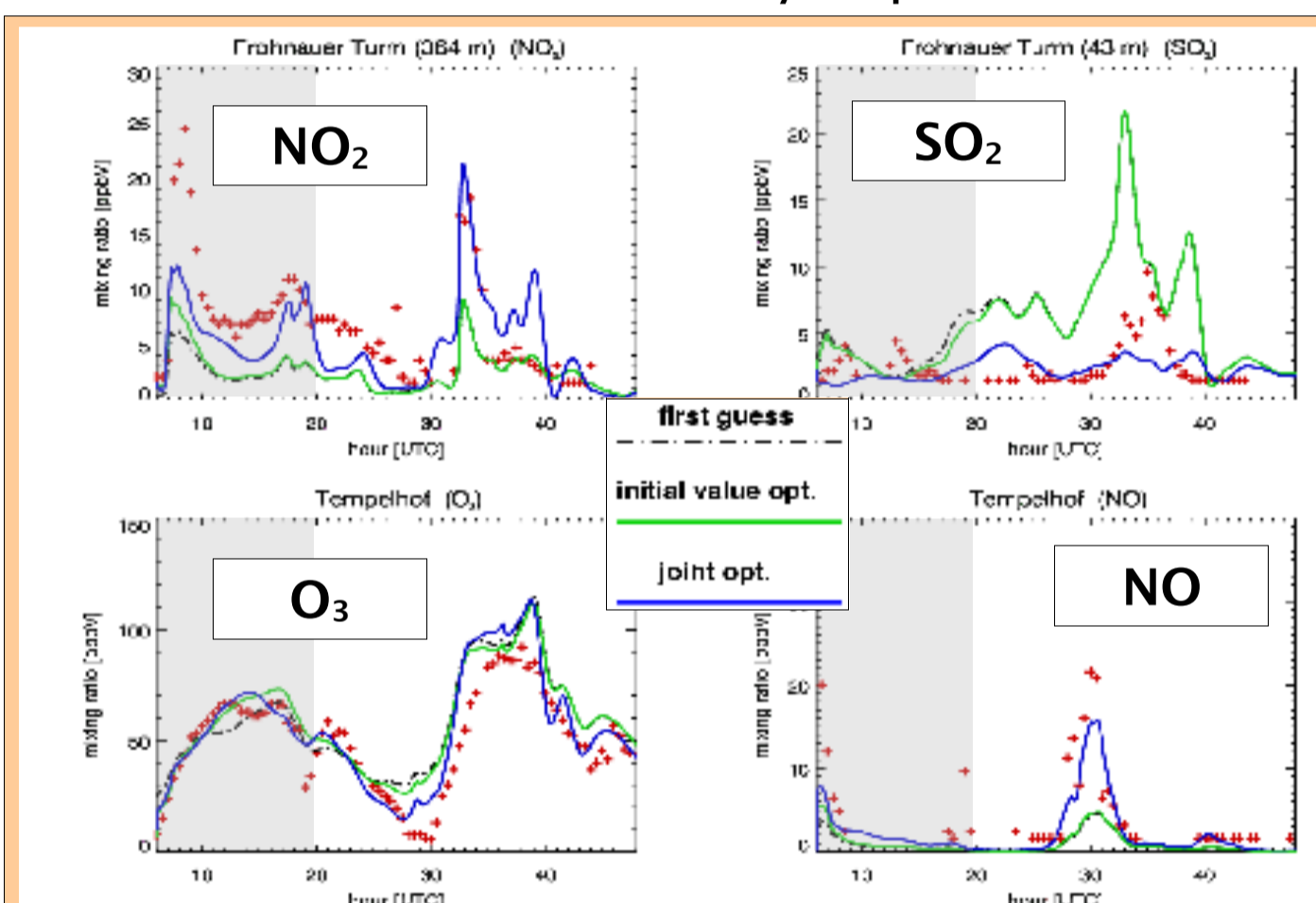


Figure 4: Time series for nest 1. Forecast improvements for the second day for NO<sub>x</sub> are only possible using joint optimisation of initial values and emission rates. Shaded region: assimilation window.

### BERLIOZ assimilation

The spatially and timely dense observational data of the BERLIOZ campaign (BERlin Ozone experiment, July and August 1998) has been used for an episodic simulation (July 18–21, 1998) with a nested data assimilation technique. The assimilation procedure was supported by a suite of improvements, including a combined campaign and routine data stream and improved vertical resolution (in addition to nesting). Additionally available routinely gathered European measurements were used as observational basis. Assimilated species are O<sub>3</sub>, NO, NO<sub>2</sub>, CO and SO<sub>2</sub> in an assimilation window of 14 hours, from 06 UTC to 20 UTC on July 20, 1998. The nesting procedure included a coarse grid simulation with horizontal grid size of 54 km and two nested grids with a nesting ratio of three (figure 1). After assimilating available measurements on the coarse grid, optimised model states were used to provide initial and boundary values as well as emission rates for the respective nested run. Significant benefits for ozone on the coarse grid are shown in figure 2 for the assimilation period. Further improvements required higher spatial resolution. First indication for nesting successes are shown in figure 3. Bias and root mean square error (RMS) for CO and NO<sub>2</sub> are significantly reduced due to refining the grid down to 6 by 6 km.

The current parallel implementation of the adjoint EURAD-CTM allows to optimise initial values as well as emission rates. For the BERLIOZ assimilation the combined optimisation of initial state and emission rates has been applied as well as optimisation of initial values only. Figure 4 shows time series within nest 1 (N1) comparing analysis results of joint optimisation with initial value optimisation. Especially for NO<sub>2</sub> and NO the combined optimisation leads to a very good subsequent forecast skill during the second day, which is used as a quality control. On nesting level 2 (N2) the time series also show the same improved skills during the assimilation window (gray shaded area) and the subsequent forecast for the joint optimisation (figure 5). The vertical structure is improved as well, shown by the tethered balloon (figure 5).

The optimisation of emission rates introduces scaling factors for the emitted amount of each species and grid cell. These factors are passed from each mother domain to its nest. Figure 6, in which emission factors for SO<sub>2</sub> and Xylene on nesting level 2 are shown, demonstrates the mechanism: the different optimisation stages in terms of coarse grid, nest 1 and nest 2 boxes are obvious. Each nest only slightly refines the previous determined scaling factors leading to a strong improvement of forecast skill for emitted species.

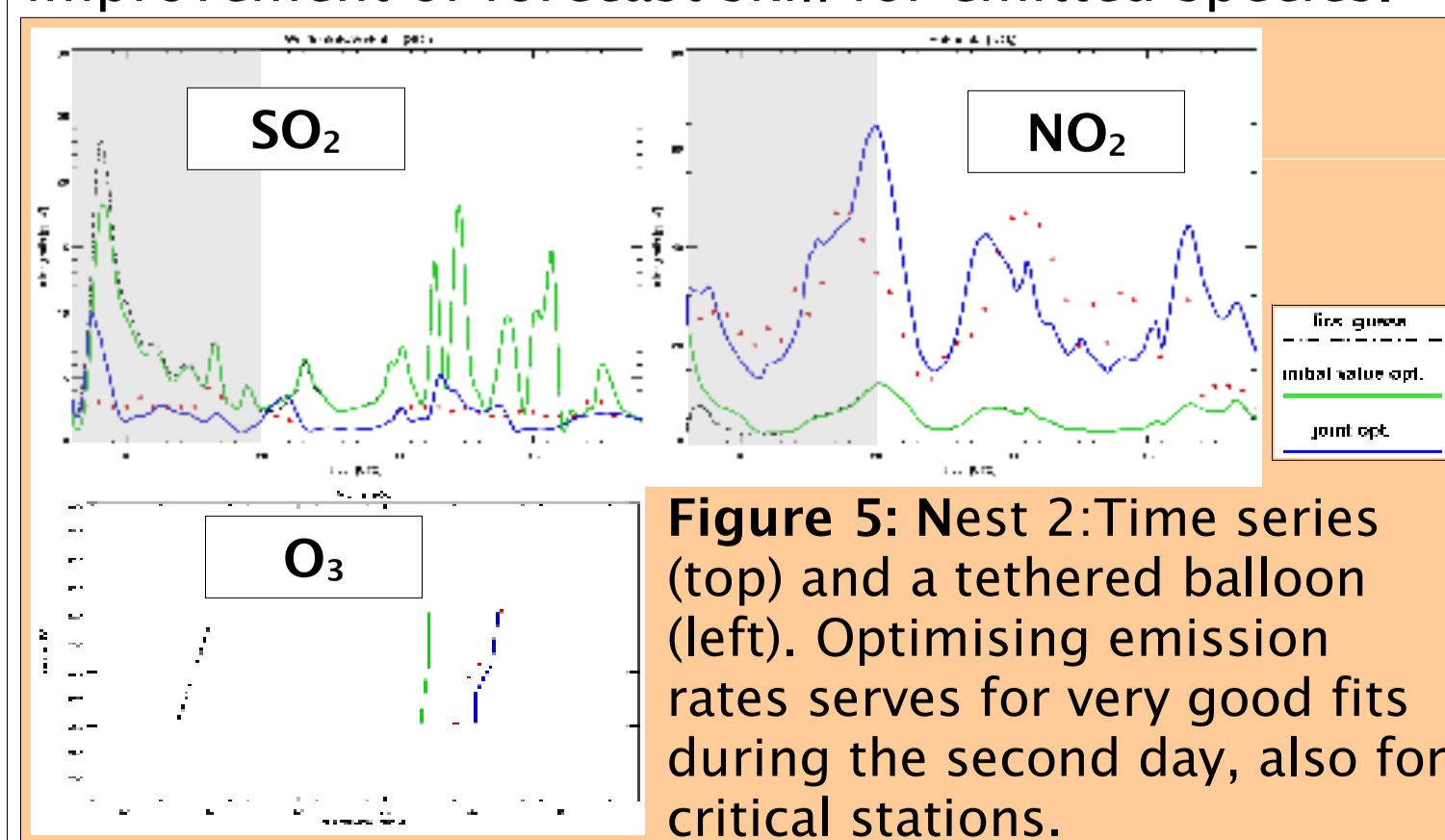


Figure 5: Nest 2: Time series (top) and a tethered balloon (left). Optimising emission rates serves for very good fits during the second day, also for critical stations.

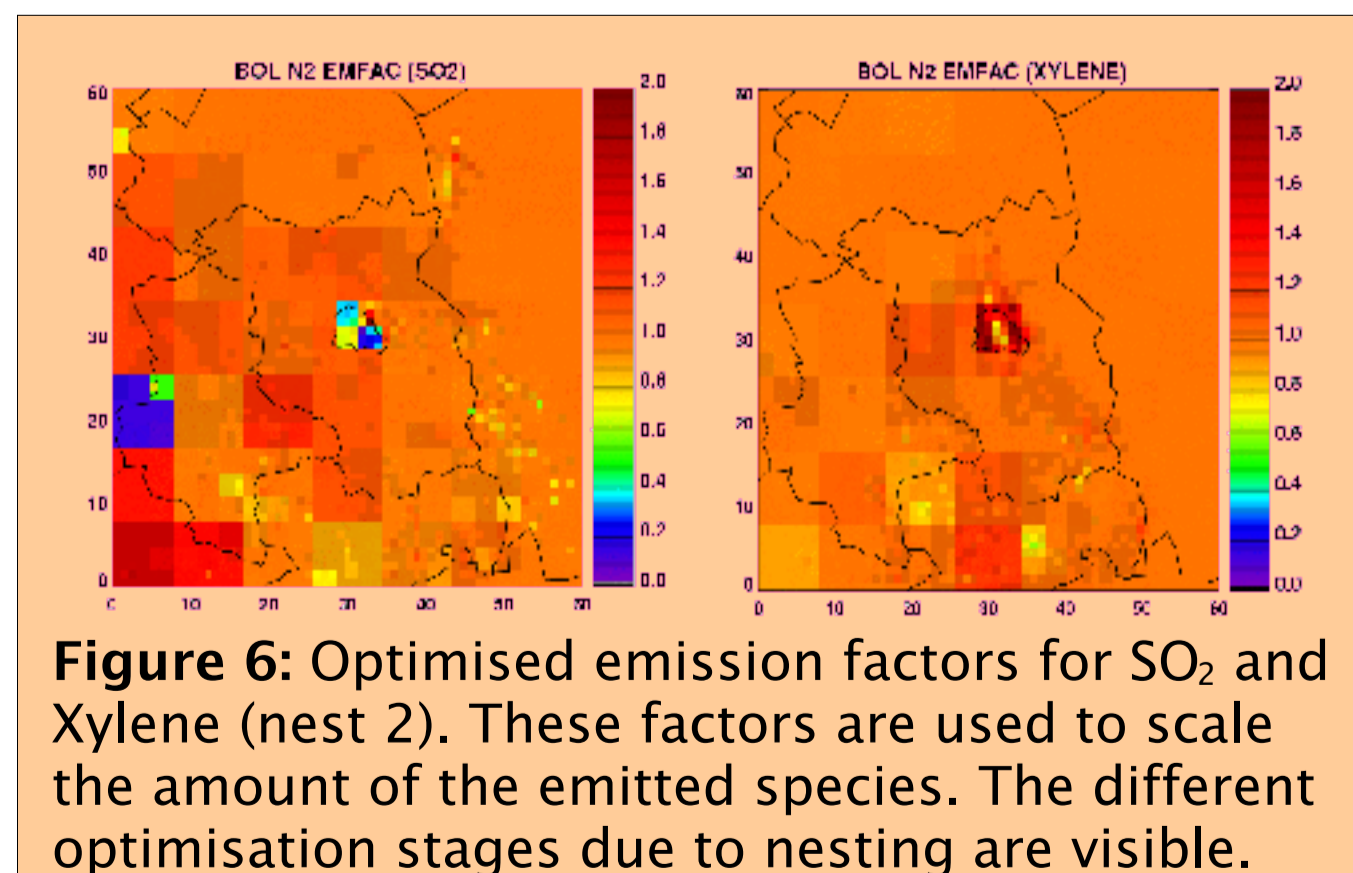


Figure 6: Optimised emission factors for SO<sub>2</sub> and Xylene (nest 2). These factors are used to scale the amount of the emitted species. The different optimisation stages due to nesting are visible.

A more detailed view in assimilation statistics is given in table 1: The 4d-var technique is governed by a cost function (figure 7), that measures the difference between model states and observations. The reduced costs due to assimilation after each nest step are compared to costs without assimilation.

**Conclusions:** It turned out that the finest nest with 6 km resolution delivers the best results. However, unlike in traditional data assimilation, the feature of joint emission rate + initial value optimisation appears to be a prerequisite for skillful forecast of emitted species. Both grid refinement down to 6 km and the emission rate optimisation are especially crucial features for improved forecast of NO and NO<sub>2</sub> but also for O<sub>3</sub>, SO<sub>2</sub> and CO. The verification against forecast improvement can be taken as a posteriori validation of flux estimates of emitted species, which is a major project objective.

### CONTRACE assimilation

The first CONTRACE episode with a special flight on Nov 14, 2001 was selected for upper tropospheric assimilation, with warm conveyor belt features induced by cyclone dynamics. The vertical grid structure has been refined for that height region, having now 26 layers. Horizontal grid size is 125 km. A spin-up period of four days has been performed. Campaign data was extended by routinely gathered European observations (figure 8). Assimilated species are O<sub>3</sub>, NO, NO<sub>2</sub>, SO<sub>2</sub>, H<sub>2</sub>O<sub>2</sub>, HCHO and CO. Figure 9 shows forecast improvements for the data of the first flight A during the morning of Nov 14. Initial values have been optimised for midnight (00:00 UTC) to ensure a daily consistent chemical model state. Especially ozone and CO show very good enhancements due to assimilation while all assimilated species are improved.

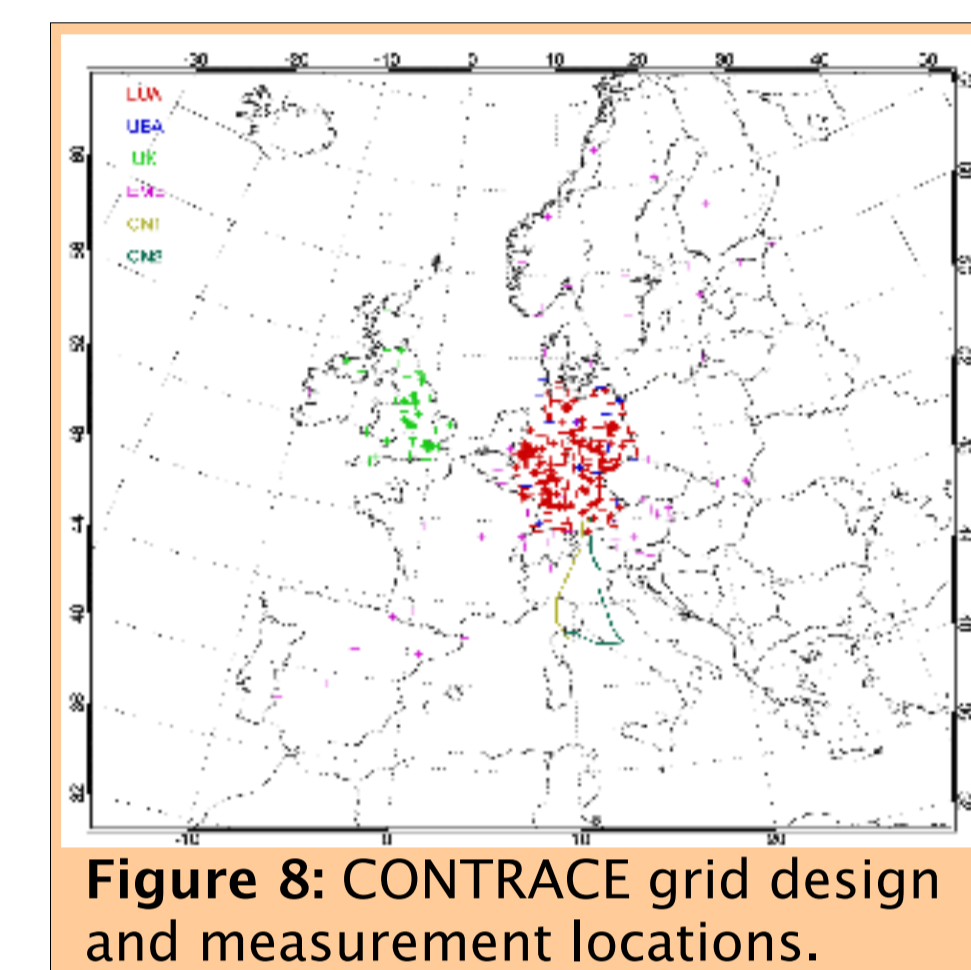


Figure 8: CONTRACE grid design and measurement locations.

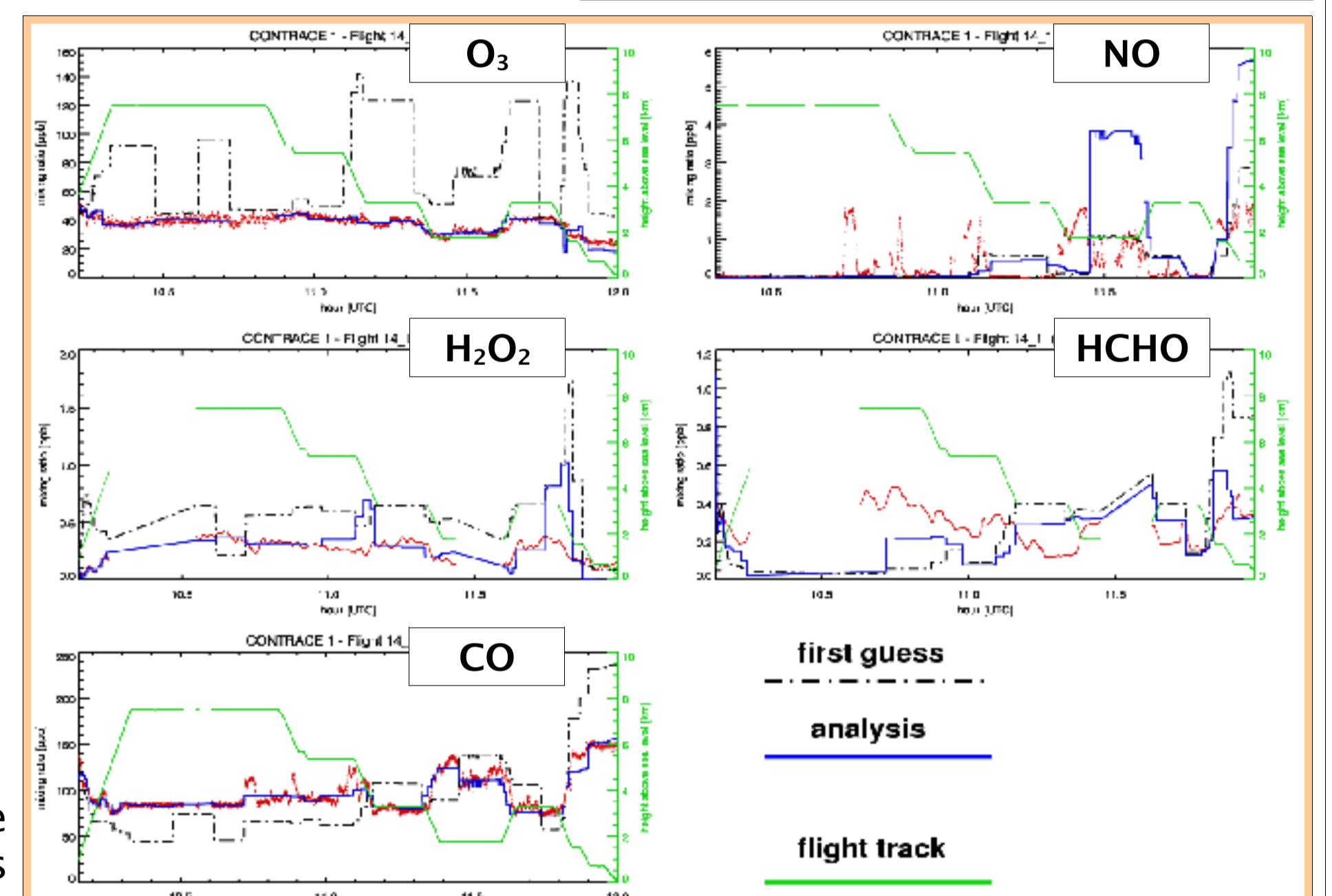


Figure 9: CONTRACE time series flight A (south bound) for O<sub>3</sub>, NO, H<sub>2</sub>O<sub>2</sub>, HCHO and CO. Joint optimisation of emission rates and initial values for midnight (00 UTC).

### SPURT assimilation

SPURT campaigns aim to observe the state of the UT/LS as a means of understanding the relevant processes. Measurements are based on airborne in situ sensors flown at height levels between 7 to 13 km. The model grid configuration is as with CONTRACE. From the suite of observations ozone and CO are taken in this assimilation procedure resulting from a north bound cruise (figure 10). The assimilation procedure was run with initial value optimisation mode, starting at 00:00 UTC. It can be seen from figure 11, that, beginning with a rough climatological first guess, a considerable performance improvement can be claimed. Chemical signatures of UT/LS streamer features can be resimulated after the assimilation process with considerable success.

### Special Acknowledgement:

We gratefully acknowledge providing campaign data and the instructive discussions with the groups involved in **CONTRACE** and **SPURT**!

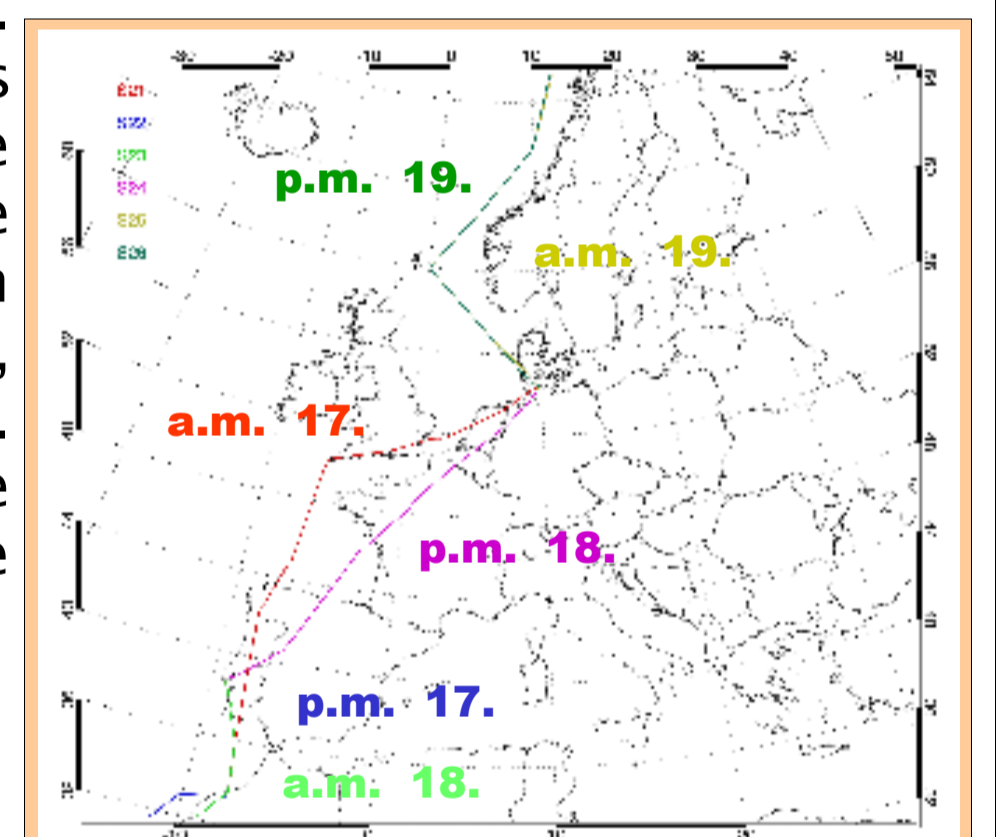


Figure 10: SPURT domain and flight tracks.

### SATEC4D post-AFO 2000 application

Developments of the project will directly feed into an operational air quality forecast system, which will be established in the framework of European GMES activities.

### Conclusions

4D-var is shown to be able to improve not only forecast skill considerably but also to find more reliable flux estimates if nesting techniques are applied and emission rates are optimised along with state variables. The nesting approach demonstrates convergence for emission rates resulting in a better analysis. The aircraft campaigns could be analysed by coarse grid assimilation. For a more detailed view the following future steps are envisaged for SPURT and CONTRACE:

- gathering additional observations for campaign times (SPURT),
- refining horizontal grid structure while extending domain (SPURT & CONTRACE),
- adjusting assimilation technique features (covariance matrices, influence radii etc.).

### A final example of mesoscale satellite data assimilation

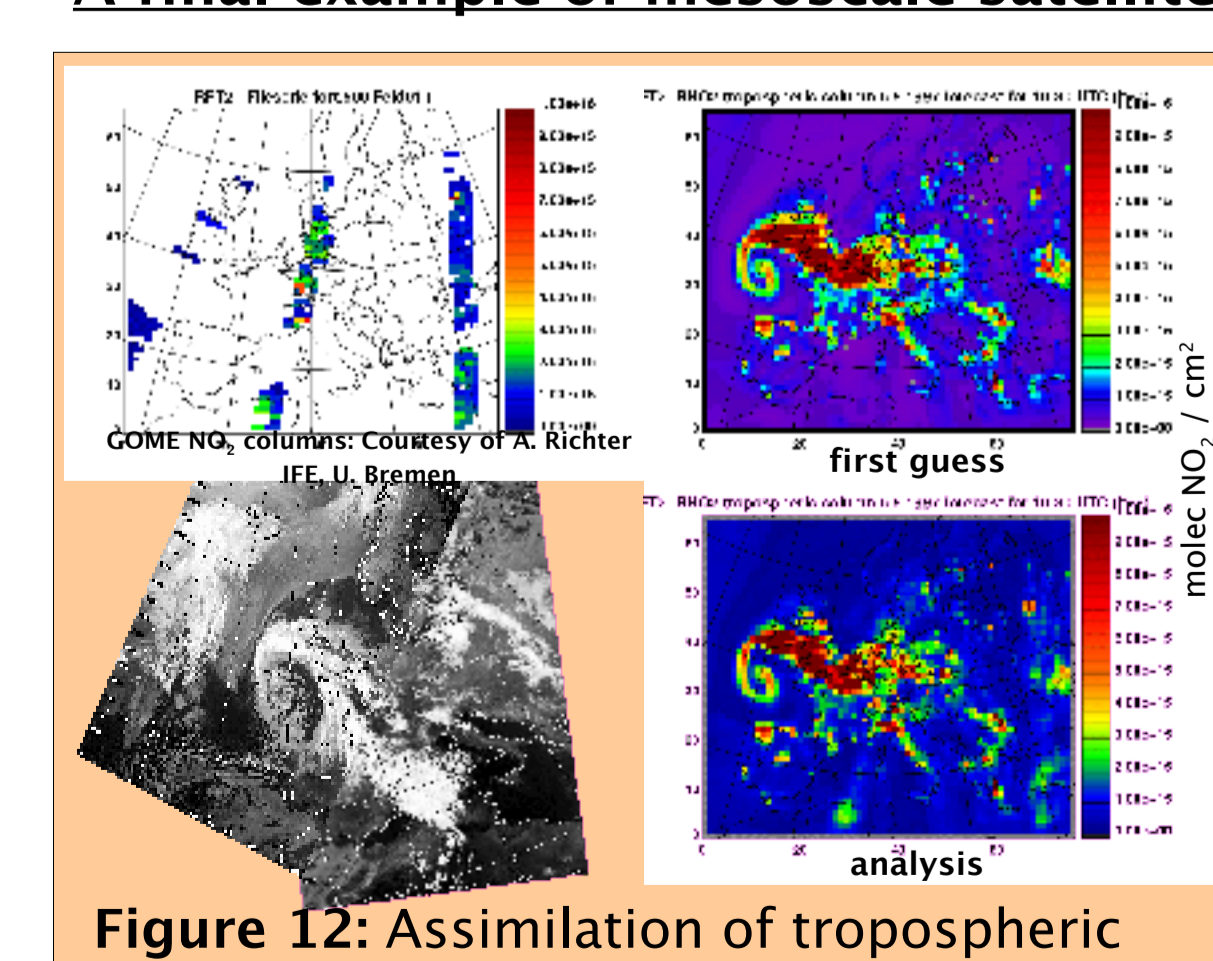


Figure 12: Assimilation of tropospheric GOME NO<sub>2</sub> columns.

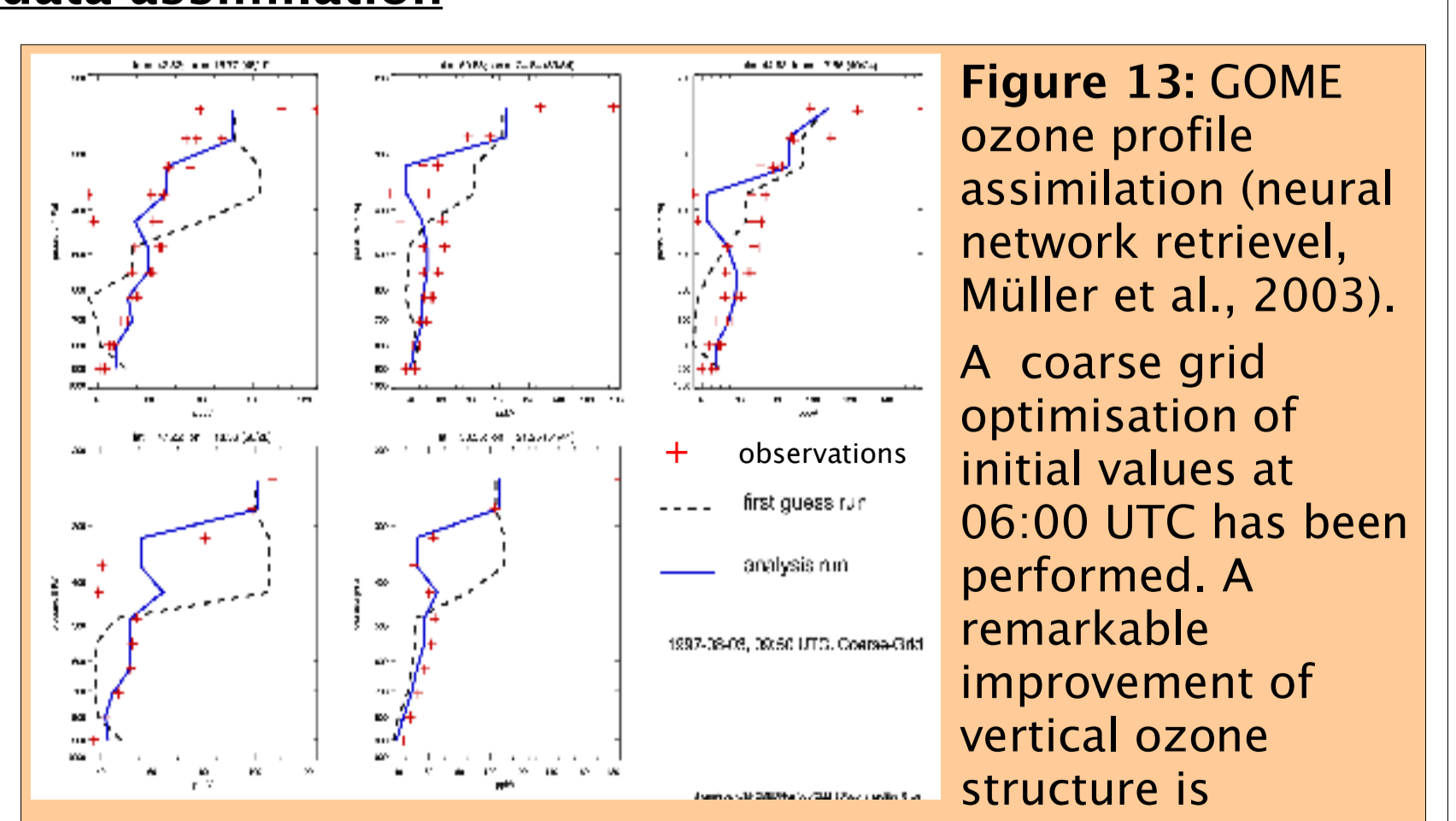


Figure 13: GOME ozone profile assimilation (neural network retrieval, Müller et al., 2003). A coarse grid optimisation of initial values at 06:00 UTC has been performed. A remarkable improvement of vertical ozone structure is achieved for all grid cells at 09:50 UTC.

	observations	costs J <sub>0</sub> (1 <sup>st</sup> guess)	costs J <sub>n</sub> (result)	J <sub>n</sub> /J <sub>0</sub>
CG				
CG+	30607	38501	15372	0.40
N1				
CG- N1	-	43306	(21182)	(0.49)
CG+ N1	27335	34157	21182	0.62
N2				
CG- N1- N2	-	35908	(16986)	(0.47)
CG+ N1- N2	-	30874	(16986)	(0.55)
CG+ N1+ N2	11196	27498	16986	0.62

**Table 1:** Minimisation statistics. (- = no assimilation, + = assimilation) Assimilating on coarse grid leads to a better first guess on each nest and so on (green circles). Overall cost reduction due to assimilation are 60% (CG), 51% (N1) and 53% (N2) (red circles).

$$J = \frac{1}{2} (y_0 - x_0^T N^{-1} (y_0 - x_0^T)) + \frac{1}{2} \sum_{i=1}^n (H_i x_i - y_i^T)^T N_i^{-1} (H_i x_i - y_i^T)$$

$x_i$ : model state at time  $t_i$  ( $= \Delta t_i(x_{i-1})$ )  
 $x_0^T$ : background model state  
 $y_i^T$ : observation at time  $t_i$   
 $B_i$ : background-covariance matrices  
 $R_i$ : covariance matrix  
 $N_i$ : representativeness and measuring errors  
 $H_i$ : observation operator

Figure 7: Cost function. See text.



The following institutions are gratefully acknowledged for giving access to their observational data: German Weather Service (DWD); Federal Agency of Environment (UBA) – Germany; Federal Agency of Environment (UBA) – Austria; Federal Agency of Environment, Forests and Landscape (BUWal) – Switzerland; National Air Quality Information Archive – United Kingdom; EMEP; Rijksinstituut voor Volksgezondheid en Milieuhygiene (RIVM) – The Netherlands; MPI for Chemistry, University of Mainz – Germany; Research Centre Jülich, ICG-I – Germany; German Aerospace Centre, IPA, Oberpfaffenhofen – Germany; German Aerospace Centre, DFD – Oberpfaffenhofen – Germany; IMK-IFU, Garmisch-Partenkirchen – Germany; MPI-K, Heidelberg – Germany; IFE, University of Bremen – Germany.

We also gratefully acknowledge the computational support by the Central Institute for Applied Mathematics (ZAM) at the Research Centre Jülich – Germany.

